

Macroscopic models for heterogeneous reactions in porous media

Federico Municchi^{a,*}, Matteo Icardi^a

^a*School of Mathematical Sciences, University of Nottingham, Nottingham, UK*

Abstract

Derivation of coarse grained models for advection-diffusion processes in the presence of dominant surface reactions using homogenisation theory or volume averaging is often deemed unfeasible [1, 2] due to the strong coupling between scales that characterise such systems. In this work, we show how this problem can be circumvented by applying and extending the methods presented in Allaire and Raphael [3], Mauri [4]. Such process gives rise to a set of cell problems that we solve using the open source finite volume library OpenFOAM[®]. We provide details on the implementation in OpenFOAM[®] and results for two-dimensional periodic arrays of spheres, for different Péclet and surface Damköhler numbers, are compared to fully resolved numerical simulations.

Keywords: Homogenisation, Reactive Transport, Upscaling, Pore-scale simulation, OpenFOAM[®]

Contents

1	Introduction	2
1.1	Problem statement and dimensionless governing equations	2
1.2	Homogenisation via two-scale asymptotics	3
1.2.1	The failure of two-scale asymptotics	4
1.3	Goals and outline	4
2	Upscaling via scale decomposition	4
2.1	Problem decomposition	5
2.2	Two-scales asymptotics with drift	6
2.3	Terms of order $O(1)$	8
2.4	Extension to inhomogeneous boundary conditions	9
3	Numerical implementation of the upscaling method	10
3.1	Overall structure of the algorithm	10
3.2	Power method for the spectral problem	10
3.3	Numerical solution of the corrector problem	12
4	Numerical results	12
4.1	Verification	12
4.2	Parametric study - homogenisation of flow through reactive FCC array of spheres	13
5	Conclusions	15

*Corresponding author
Email address: federico.municchi@nottingham.ac.uk (Federico Municchi)

1. Introduction

Porous media are relevant to a wide range of chemical processes (for example drying of paper pulp or flow through catalysts) and applications (subsurface flows, CO_2 storage, nuclear waste management, etc.) [5]. However, the study of transport phenomena in porous media is complicated by the broad range of excited space and time scales, which results in large (almost always unaffordable) computational requirements when simulating such systems at industrial or natural scales. Therefore, any precise simulation describing the local, pore-scale, phenomena would be of little practical applicability, without a robust methodology that leads to upscaled models.

In the following, will use the terms 'upscaling' to describe the procedure leading to 'upscaled models' where the 'fast' (high wave number) components of the unknown fields are averaged out. Notice that often the terms 'spatial filtering' [6] or 'coarse graining' [7] are also employed in literature with a similar meaning.

A variety of methods can be employed to perform this upscaling procedure: asymptotic homogenisation [8, 9, 10] is a powerful and versatile tool for the upscaling of transport and reaction equations in porous and heterogeneous media. For example, Taylor dispersion in porous media has been approached in this way [11] and there have been attempts to account for of heterogeneous (surface) reaction [12, 13].

1.1. Problem statement and dimensionless governing equations

Consider a porous medium occupying a region of space $\hat{\Omega}$ associated with a characteristic length L . We also assume that $\hat{\Omega}$ can be thought as composed of spatially repeating unit cells $\hat{\mathcal{Y}}$ with characteristic length: $\ell = \varepsilon L \ll 1$. Each unit cell $\hat{\mathcal{Y}}$ is then given by the union $\hat{\mathcal{Y}} = \hat{\mathcal{Y}}_f \cup \hat{\mathcal{Y}}_s$, where $\hat{\mathcal{Y}}_f$ and $\hat{\mathcal{Y}}_s$ are the fluid and solid regions of $\hat{\mathcal{Y}}$ respectively, separated by an interface $\hat{\Gamma}$. Clearly, $\hat{\mathcal{Y}}_f$ is generally not simply connected, while $\hat{\mathcal{Y}}_s$ is a disconnected domain (for example, it may represent grains inside the porous medium). Furthermore, we consider a fluid flow in $\hat{\mathcal{Y}}_f$. In the particular case in which such flow is well described by the Stokes equations (i.e., incompressible, low Reynolds number), it has been shown that the homogenisation procedure leads to the Darcy equation [11]. Therefore, in this work we will only concern with scalar transport, and assume that the velocity field is prescribed.

We consider a generic (dimensional) scalar field $\hat{c}(\mathbf{x}, t)$ defined in the fluid region $\hat{\Omega}_f$ given by the $\hat{\mathcal{Y}}_f$ of each cell (we will not consider the case of conjugate transport in both regions that will be studied in future works[14]) that obeys the advection-diffusion equation:

$$\begin{cases} \frac{\partial \hat{c}}{\partial \hat{t}} + \hat{\mathbf{v}} \cdot (\hat{\mathbf{v}} \hat{c}) = \hat{\mathbf{v}} \cdot (\mathcal{D} \hat{\nabla} \hat{c}) & \hat{\mathbf{x}} \in \hat{\Omega}_f \\ \mathcal{D} \hat{\nabla} \hat{c} \cdot \mathbf{n} = -\kappa \hat{c} + \hat{g} & \hat{\mathbf{x}} \in \hat{\Gamma}_\Omega \end{cases} \quad (1)$$

where \mathcal{D} is a diffusion coefficient, $\hat{\mathbf{v}}(\hat{\mathbf{x}})$ a solenoidal velocity field and $\hat{g}(\hat{\mathbf{x}})$ is a known forcing term in the boundary conditions. The mixed boundary condition on the solid surface $\hat{\Gamma}_\Omega$ (the union of the interfaces $\hat{\Gamma}$ of all the unit cells) is, for the limit $\kappa \rightarrow \infty$, equivalent to a homogeneous Dirichlet condition.

Equation 1 should be provided with a proper set of *external* boundary conditions (e.g., inlet/outlet). Since such boundary conditions are specific for each problem and should not concern the homogenisation procedure, we will not explicitly state them. However, it is important to notice that homogenisation fails in case the external boundary conditions play a significant role at the scale ℓ since the model with periodic unit cells $\hat{\mathcal{Y}}$ would fail to be a realistic and mathematically consistent description of the porous medium as outlined in Auriault and Adler [11].

It is important to notice that we limit here to the case of periodic and non-moving porous media. However, some of these ideas can be extended to stochastic stationary multiscale random media, with Fourier/Bloch [15, 16] or numerical sampling [17] approaches, and to slowly varying or quasi-periodic media [18, 19]. These extensions will be considered in future studies.

We now introduce a set of dimensionless quantities:

$$\mathbf{x} = \frac{\hat{\mathbf{x}}}{L}; \quad \mathbf{v} = \frac{\hat{\mathbf{v}}}{U} \quad c = \frac{\hat{c}}{c_0}, \quad \hat{t} = \frac{L^2}{\mathcal{D}} t, \quad g = \frac{\hat{g}}{\kappa c_0} \quad (2)$$

When the dimensionless quantities are substituted into equation 1, two dimensionless number arise:

- The Péclet number:

$$\text{Pe} = \frac{U\ell}{\mathcal{D}} \quad (3)$$

Which represents the ratio between inertial and diffusion time scales the microscale.

- The second Damköhler number:

$$\text{Da}_{\text{II}} = \frac{\kappa\ell}{\mathcal{D}} \quad (4)$$

Which gives the ratio between the reaction and diffusion time scales at the microscale.

Thus, recalling that $\varepsilon = \ell/L$, can write the advection-diffusion problem in dimensionless form:

$$\begin{cases} \frac{\partial c}{\partial t} + \nabla \cdot (\varepsilon^{-1} \text{Pev}c - \nabla c) = 0 & \mathbf{x} \in \Omega \\ \nabla c \cdot \mathbf{n} = \varepsilon^{-1} \text{Da}_{\text{II}}(g - c) & \mathbf{x} \in \Gamma_{\Omega} \end{cases} \quad (5)$$

1.2. Homogenisation via two-scale asymptotics

Following the standard two-scale asymptotic homogenisation method [20], we introduce a "fast" spatial variable \mathbf{y} defined as follows:

$$\mathbf{y} = \frac{\mathbf{x}}{\varepsilon} \quad (6)$$

Then, c is represented as $c(\mathbf{x}, t) = c(\mathbf{x}, \mathbf{y}, t)$ and expanded into an asymptotic series of ε

$$c(\mathbf{x}, \mathbf{y}, t) = \sum_{m=0}^{\infty} \varepsilon^m c_m(\mathbf{x}, \mathbf{y}, t) \quad (7)$$

Using 6 we obtain the following differentiation rule:

$$\nabla c = \nabla_{\mathbf{x}} c + \varepsilon^{-1} \nabla_{\mathbf{y}} c \quad (8)$$

Furthermore, we consider the case of equally important advection and diffusion at large scales $\text{Pe} = \text{Pe}_L = \mathcal{O}(1)$ without any loss of generality.

Substituting into equation 5 and collecting terms of the same order ε we obtain:

$$\begin{aligned} & \varepsilon^{-2} \left\{ \nabla_{\mathbf{y}} \cdot (\text{Pev}c_0 - \nabla_{\mathbf{y}}c_0) \right\} + \\ & \varepsilon^{-1} \left\{ \nabla_{\mathbf{x}} \cdot (\text{Pev}c_0 - \nabla_{\mathbf{y}}c_0) - \nabla_{\mathbf{y}} \cdot [(\nabla_{\mathbf{x}}c_0 + \nabla_{\mathbf{y}}c_1 - \text{Pev}c_1)] \right\} + \\ & \varepsilon^0 \left\{ \frac{\partial c_0}{\partial t} - \nabla_{\mathbf{x}} \cdot [(\nabla_{\mathbf{x}}c_0 + \nabla_{\mathbf{y}}c_1)] - \nabla_{\mathbf{y}} \cdot [(\nabla_{\mathbf{x}}c_1 + \nabla_{\mathbf{y}}c_2)] \right\} + \\ & \quad + \text{Pe} \nabla_{\mathbf{x}} \cdot (vc_1) \Big\} = \mathcal{O}(\varepsilon) \end{aligned}$$

We apply the same expansion to the boundary condition in Γ_{Ω} for the homogeneous case $g = 0$:

$$(\nabla_{\mathbf{x}} + \varepsilon^{-1} \nabla_{\mathbf{y}})(c_0 + \varepsilon^1 c_1 + \varepsilon^2 c_2) \cdot \mathbf{n} = -\varepsilon^{-1} \text{Da}_{\text{II}}(c_0 + \varepsilon^1 c_1 + \varepsilon^2 c_2) + \mathcal{O}(\varepsilon^3) \quad \mathbf{y} \in \Gamma_{\Omega} \quad (9)$$

1.2.1. The failure of two-scale asymptotics

Collecting terms of order $O(\varepsilon^{-2})$ in equation 9 and (9), and considering that for an incompressible fluid $\nabla_{\mathbf{y}} \cdot \mathbf{v} = 0$, we obtain a problem in the unit cell:

$$\begin{cases} \nabla_{\mathbf{y}} \cdot (-\nabla_{\mathbf{y}} c_0) = 0 & \mathbf{y} \in \mathcal{Y}_f \\ \nabla_{\mathbf{y}} c_0 \cdot \mathbf{n} = \text{Da}_{\text{II}} c_0 & \mathbf{y} \in \Gamma \end{cases} \quad (10)$$

Generally, homogenisation works if the equation for the lowest order gives that the first term of the asymptotic expansion is independent of \mathbf{y} , i.e., $c_0 = c_0(\mathbf{x}, t)$. This allows the subsequent order equations to simplify and to finally perform volume averaging to obtain a well defined effective concentration. For example, in the case of $\text{Da}_{\text{II}} = 0$ (impremeable non reactive walls), the resulting homogeneous Neumann boundary condition would ensure that no dependence on \mathbf{y} is retained in c_0 . Due to the geometry of the unit cell (periodicity and internal boundary), equation 10 is satisfied (without any dependence on the microscale coordinate \mathbf{y}) only for the trivial case $c_0 = 0$ everywhere, thus removing the leading order term from the asymptotic expansion. This phenomenon is essentially triggered by a lack of separation of scales, i.e. the leading order of the asymptotic expansion directly depends upon the boundary conditions on Γ . Therefore, the problem can not be homogenised anymore using this technique.

1.3. Goals and outline

In this work we show how homogenised equations can be derived in the case of reactive transport by mean of the technique developed by Allaire and Raphael [3] in the case of homogeneous reactions and we generalised it to include some simple non-homogeneous boundary conditions often find in engineering applications. Furthermore, we describe how the resulting upscaling algorithm can be implemented in the opensource C++ finite volume library OpenFOAM®. This work is structured as follows: in Section 2 we present the approach of Allaire and Raphael and its extension. In section 3 we detail the numerical algorithm, and in section 4 we show how the method compares against numerical predictions and present some results for periodic arrays of spheres. Finally, we present conclusions and outlook in section 5.

2. Upscaling via scale decomposition

In order to upscale the advection-diffusion equation with reactive boundary conditions, we apply a decomposition method where the scalar field is appropriately separated into terms that account for exchange processes at different scales.

In order to shorten our notation, we introduce the steady advection-diffusion operator:

$$\mathcal{L} = \nabla \cdot [\text{Pev}(\mathbf{x}) - \nabla] \quad (11)$$

That allows to rewrite equation (5) in the more succinct way:

$$\begin{cases} \left(\frac{\partial}{\partial t} + \mathcal{L} \right) c(\mathbf{x}, t) = 0 & \forall \mathbf{x} \in \Omega \\ \nabla c(\mathbf{x}, t) \cdot \mathbf{n} = \text{Da}_{\text{II}} c(\mathbf{x}, t), & \forall \mathbf{x} \in \Gamma_{\Omega} \end{cases} \quad (12)$$

Again, we do not consider other ‘‘external’’ boundary conditions, as if we were considering a ‘‘bulk’’ region where the dynamics is completely determined by the boundary conditions in Γ_{Ω} .

2.1. Problem decomposition

We employ the geometrical periodicity of the system to separate $c(\mathbf{x}, t)$ into a function $\phi(\mathbf{x}, t)$ periodic in \mathcal{Y} and another function $\omega(\mathbf{x}, t)$, which is not necessarily periodic. Therefore we write:

$$c(\mathbf{x}, t) = \phi(\mathbf{x}) \omega(\mathbf{x}, t) \quad (13)$$

The aim of decomposition 13 is to separate that part of $c(\mathbf{x}, t)$ that operates the exchange between Ω and Γ_Ω from the part that operates the transport over long distances. We therefore choose ϕ as eigenfunction of \mathcal{L} in \mathcal{Y} , which satisfies:

$$\begin{cases} \mathcal{L}\phi(\mathbf{x}) = \lambda\phi(\mathbf{x}), & \forall \mathbf{x} \in \mathcal{Y}_f \\ \nabla\phi(\mathbf{x}) \cdot \mathbf{n} = \text{Da}_\Pi\phi(\mathbf{x}), & \forall \mathbf{x} \in \Gamma \end{cases} \quad (14)$$

Therefore, $\omega(\mathbf{x}, t)$ can be thought as a reduced concentration, which compensates for the arbitrariness of our choice of ϕ .

Substituting back equation (13) into $\mathcal{L}c$ (dropping the dependence on \mathbf{x} and t) we obtain:

$$\begin{aligned} \mathcal{L}(\phi\omega) &= \nabla \cdot [\text{Pev}\phi\omega - \nabla(\phi\omega)] \\ &= \nabla \cdot (\text{Pev}\phi\omega - \phi\nabla\omega - \omega\nabla\phi) \\ &= \phi\nabla \cdot (\text{Pev} - \nabla)\omega + \omega\nabla \cdot (\text{Pev} - \nabla)\phi - \nabla\phi \cdot \nabla\omega \\ &= \phi\mathcal{L}\omega + \omega\mathcal{L}\phi - \nabla\phi \cdot \nabla\omega \\ &= \phi\mathcal{L}\omega + \omega\lambda\phi - \nabla\phi \cdot \nabla\omega \end{aligned} \quad (15)$$

While the term $\omega\lambda\phi$ can be removed by mean of an appropriate transformation, last term on the right-hand-side of equation (15) involving the dot product of $\nabla\phi$ and $\nabla\omega$ requires particular care. In order to recast the problem in a more familiar way, we introduce the adjoint problem:

$$\begin{cases} \mathcal{L}^\dagger\phi^\dagger(\mathbf{x}) = \lambda^\dagger\phi^\dagger(\mathbf{x}), & \forall \mathbf{x} \in \mathcal{Y}_f \\ \nabla\phi^\dagger(\mathbf{x}) \cdot \mathbf{n} = \text{Da}_\Pi\phi^\dagger(\mathbf{x}), & \forall \mathbf{x} \in \Gamma \end{cases} \quad (16)$$

Where $\mathcal{L}^\dagger = -\nabla \cdot [\text{Pev}(\mathbf{x}) + \nabla]$. We therefore employ the adjoint function ϕ^\dagger to obtain an equation for ω :

$$\begin{aligned} \phi^\dagger\mathcal{L}(\phi\omega) &= \phi^\dagger\nabla \cdot (\text{Pev}\phi\omega - \phi\nabla\omega - \omega\nabla\phi) \\ &= \nabla \cdot (\text{Pev}\phi\phi^\dagger - \omega\phi^\dagger\phi\nabla\omega - \phi^\dagger\nabla\phi\omega) \\ &\quad + (\phi\nabla\omega + \omega\nabla\phi) \cdot \nabla\phi^\dagger - \omega\phi\nabla \cdot (\text{Pev}\phi^\dagger) \\ &= \nabla \cdot (\text{Pev}\phi\phi^\dagger - \omega\phi^\dagger\phi\nabla\omega - \phi^\dagger\nabla\phi\omega + \nabla\phi^\dagger\phi\omega) \\ &\quad - \omega\phi\nabla \cdot (\text{Pev}\phi^\dagger + \nabla\phi^\dagger) \\ &= \nabla \cdot (\text{Pev}^*\nabla\omega - \beta\nabla\omega) + \lambda\beta\omega \end{aligned} \quad (17)$$

Where we introduced a dimensionless coefficient $\beta(\mathbf{x}) = \phi\phi^\dagger$ and a new velocity field:

$$\mathbf{v}^* = \beta \left(\mathbf{v} - \frac{\nabla\phi}{\phi} + \frac{\nabla\phi^\dagger}{\phi^\dagger} \right) = \beta\mathbf{v}^+ \quad (18)$$

Where \mathbf{v}^+ is the original velocity field plus the additional pseudo velocities arising from the spectral decomposition.

Remark 1. *The new velocity field \mathbf{v}^* is divergence-free:*

$$\begin{aligned}
\nabla \cdot \mathbf{v}^* &= \nabla \cdot (\mathbf{v}\phi\phi^\dagger + \nabla\phi^\dagger D\phi - \phi^\dagger D\nabla\phi) \\
&= \phi\nabla \cdot (\mathbf{v}\phi^\dagger + D\nabla\phi^\dagger) + \phi^\dagger\nabla \cdot (\mathbf{v}\phi - D\nabla\phi) \\
&= -\phi\phi^\dagger\lambda + \phi\phi^\dagger\lambda \\
&= 0
\end{aligned} \tag{19}$$

Therefore, we can define a new advection-diffusion operator:

$$\mathcal{L}^* = \nabla \cdot [\mathbf{v}^*(\mathbf{x}) - \beta(\mathbf{x})\nabla] \tag{20}$$

and the equation for ω then reads:

$$\left[\beta \left(\frac{\partial}{\partial t} + \lambda \right) + \mathcal{L}^* \right] \omega = 0 \tag{21}$$

It is clear that equation (21) can be further simplified by mean of one additional transformation which takes into account the fast time scale related to λ :

$$\omega(\mathbf{x}, t) = e^{-\lambda t} w(\mathbf{x}, t) \rightarrow c(\mathbf{x}, t) = \phi(\mathbf{x}) e^{-\lambda t} w(\mathbf{x}, t) \tag{22}$$

Where the exponential takes into account the fast change in c due to the reaction.

Furthermore, we apply equation (22) to the boundary condition in Γ . It is easy to verify that due to our choice of ϕ , the Robin boundary condition reduces to:

$$\nabla\omega \cdot \mathbf{n} = 0 \tag{23}$$

Finally, we can write an equation for the reduced concentration w together with a proper set of boundary conditions:

$$\begin{cases} \left(\beta \frac{\partial}{\partial t} + \mathcal{L}^* \right) w = 0, & \forall \mathbf{x} \in \Omega \\ \nabla w \cdot \mathbf{n} = 0, & \forall \mathbf{x} \in \Gamma \end{cases} \tag{24}$$

Therefore, using decomposition 13 we were able to obtain an equation for the reduced concentration that has zero flux through Γ and that can be upscaled using standard two-scale asymptotics.

2.2. Two-scales asymptotics with drift

Decomposition (22) introduced an auxiliary problem in the cell \mathcal{Y}_f and clearly, the eigenfunction ϕ and the adjoint ϕ^\dagger , by construction, can only depend on the small scale spatial variable \mathbf{y} , while w can vary on both scales. It is convenient to express the solution as:

$$c(\mathbf{x}, \mathbf{y}, t) = e^{-\lambda t} \phi(\mathbf{y}) w(\mathbf{x}, \mathbf{y}, t) \tag{25}$$

Therefore, the two-scale expansion of c turns out to be fully determined by considering the two scale expansion of w only. Furthermore, the governing equation for w does not satisfy a Robin boundary condition, therefore circumventing the limitations of standard homogenisation we addressed in Section 1.

We thus expand w into an asymptotic series of ε introducing a drift in w that accounts for the fast advective transport at the microscale:

$$w(\mathbf{x} - \varepsilon^{-1}\text{Pe}\mathbf{V}^*t, \mathbf{y}, t) = \sum_{m=0}^{\infty} \varepsilon^m w_m(\mathbf{x} - \varepsilon^{-1}\text{Pe}\mathbf{V}^*t, \mathbf{y}, t) \quad (26)$$

where the velocity \mathbf{V}^* is obtained during the homogenisation procedure. Moreover, we can carry on the same procedure we adopted in Section 1 on equation 24 to obtain:

$$\begin{aligned} & \varepsilon^{-2} \left\{ \nabla_{\mathbf{y}} \cdot (\text{Pe}\mathbf{v}^*w_0 - \beta\nabla_{\mathbf{y}}w_0) \right\} + \\ & \varepsilon^{-1} \left\{ \text{Pe} \left[-\beta\mathbf{V}^* \cdot \nabla_{\mathbf{x}}w_0 + \nabla_{\mathbf{x}} \cdot (\mathbf{v}^*w_0) + \nabla_{\mathbf{y}} \cdot (\mathbf{v}^*w_1) \right] \right. \\ & \quad \left. - \nabla_{\mathbf{x}} \cdot (\beta\nabla_{\mathbf{y}}w_0) - \nabla_{\mathbf{y}} \cdot [\beta(\nabla_{\mathbf{x}}w_0 + \nabla_{\mathbf{y}}w_1)] \right\} + \\ & + \varepsilon^0 \left\{ \beta \frac{\partial w_0}{\partial t} - \beta\text{Pe}\mathbf{V}^* \cdot \nabla_{\mathbf{x}}w_1 + \text{Pe}\nabla_{\mathbf{x}} \cdot (\mathbf{v}^*w_1) + \text{Pe}\nabla_{\mathbf{y}} \cdot (\mathbf{v}^*w_2) - \right. \\ & \quad \left. - \nabla_{\mathbf{x}} \cdot [\beta(\nabla_{\mathbf{x}}w_0 + \nabla_{\mathbf{y}}w_1)] - \nabla_{\mathbf{y}} \cdot [\beta(\nabla_{\mathbf{x}}w_1 + \nabla_{\mathbf{y}}w_2)] \right\} = \mathcal{O}(\varepsilon) \end{aligned} \quad (27)$$

The internal boundary condition is also expanded:

$$(\nabla_{\mathbf{x}} + \varepsilon^{-1}\nabla_{\mathbf{y}})(w_0 + \varepsilon^1w_1 + \varepsilon^2w_2) \cdot \mathbf{n} = 0 \quad (28)$$

which corresponds to a homogeneous Neumann boundary condition for all the terms in the series.

Terms of order $\mathcal{O}(\varepsilon^{-2})$

We can now collect the leading order terms of equation (27) and (9), which correspond to terms of order $\mathcal{O}(\varepsilon^{-2})$

$$\begin{cases} \nabla_{\mathbf{y}} \cdot (\text{Pe}\mathbf{v}^*w_0 - \beta\nabla_{\mathbf{y}}w_0) = 0 & \mathbf{y} \in \Omega \\ \nabla_{\mathbf{y}}w_0 \cdot \mathbf{n} = 0 & \mathbf{y} \in \Gamma \end{cases} \quad (29)$$

This problem allows the trivial solution $w_0 = w_0(\mathbf{x}, t)$ since the homogeneous Neumann boundary condition ensures that no terms from "fast" scales appear in equations (29).

Terms of order $\mathcal{O}(\varepsilon^{-1})$

Moving on to collect terms of order $\mathcal{O}(\varepsilon^{-1})$, we obtain the following partial differential equation:

$$\begin{cases} -\text{Pe}\beta\mathbf{V}^* \cdot \nabla_{\mathbf{x}}w_0 + \text{Pe}\nabla_{\mathbf{x}} \cdot (\mathbf{v}^*w_0) + \\ \quad + \nabla_{\mathbf{y}} \cdot [\text{Pe}\mathbf{v}^*w_1 - \beta(\nabla_{\mathbf{x}}w_0 + \nabla_{\mathbf{y}}w_1)] & \mathbf{y} \in \Omega \\ (\nabla_{\mathbf{y}}w_1 + \nabla_{\mathbf{x}}w_0) \cdot \mathbf{n} = 0 & \mathbf{y} \in \Gamma \end{cases} \quad (30)$$

This equation can be integrated over the unit cell to give:

$$\left[\int_{\mathcal{Y}_f} (\beta\mathbf{V}^* - \mathbf{v}^*) \, d\mathbf{y} \right] \cdot \nabla_{\mathbf{x}}w_0 = \left[\int_{\mathcal{Y}_f} \beta(\mathbf{V}^* - \mathbf{v}^*w_0) \, d\mathbf{y} \right] \cdot \nabla_{\mathbf{x}}w_0 \quad (31)$$

Which can be simplified by assuming that the velocity field \mathbf{v} is solenoidal at the microscopic scale:

$$\mathbf{V}^* = \frac{1}{\epsilon} \int_{\mathcal{Y}_f} \mathbf{v}^+(\mathbf{y}) d\mathbf{y} = \langle \mathbf{v}^+ \rangle \quad (32)$$

Where we defined the Favre average of the velocity field $\langle \mathbf{v}^+ \rangle$ and the effective porosity ϵ as:

$$\epsilon = \int_{\mathcal{Y}_f} d\mathbf{y} \quad (33)$$

Therefore \mathbf{V}^* is the upscaled effective velocity field for the advection-diffusion-reaction problem.

We now notice that when substituting (32) into equation (30), we can express the solution w_1 as:

$$w_1 = \chi(\mathbf{y}) \cdot \nabla_{\mathbf{x}} w_0 + f_1(\mathbf{x}) \quad (34)$$

Where χ is called first order corrector and f_1 is an arbitrary function of the macroscopic coordinate.

Substituting equation (34) into equations (30) we obtain:

$$\begin{cases} -\nabla_{\mathbf{y}} \cdot [\beta(\mathbf{I} + \nabla_{\mathbf{y}} \chi)] + \text{Pe} \mathbf{v}^* \cdot (\mathbf{I} + \nabla_{\mathbf{y}} \chi) = \text{Pe} \beta \mathbf{V}^* & \mathbf{y} \in \mathcal{Y}_f \\ (\mathbf{I} + \nabla_{\mathbf{y}} \chi) \cdot \mathbf{n} = 0 & \mathbf{y} \in \Gamma \end{cases} \quad (35)$$

equations (35) are often referred as the first order cell corrector problem, since χ appears in the expressions for the effective diffusion coefficient. Notice that the first order corrector only depends on \mathbf{y} and therefore, its governing equation can be defined in the unit cell \mathcal{Y} alone.

2.3. Terms of order $O(1)$

Finally, we collect the terms of order $O(1)$ from equation (27):

$$\begin{cases} \beta \frac{\partial w_0}{\partial t} + \beta \text{Pe} (\mathbf{v}^+ - \mathbf{V}^*) \cdot \nabla_{\mathbf{x}} w_1 + \text{Pe} \nabla_{\mathbf{y}} \cdot (\mathbf{v}^* w_2) - \\ -\nabla_{\mathbf{x}} \cdot [\beta(\nabla_{\mathbf{x}} w_0 + \nabla_{\mathbf{y}} w_1)] - \nabla_{\mathbf{y}} \cdot [\beta(\nabla_{\mathbf{x}} w_1 + \nabla_{\mathbf{y}} w_2)] & \mathbf{y} \in \Omega \\ (\nabla_{\mathbf{x}} w_1 + \nabla_{\mathbf{y}} w_2) \cdot \mathbf{n} = 0 & \mathbf{y} \in \Gamma \end{cases} \quad (36)$$

equation (36) can be integrated over \mathcal{Y}_f to obtain:

$$\langle \beta \rangle \frac{\partial w_0}{\partial t} - \nabla_{\mathbf{x}} \cdot [\langle \beta(\mathbf{I} + \nabla_{\mathbf{y}} \chi + \text{Pe} \mathbf{V}^* \chi - \text{Pe} \mathbf{v}^+ \chi) \rangle \cdot \nabla_{\mathbf{x}} w_0] = 0 \quad (37)$$

Without loss of generality, we can take β such that:

$$\langle \beta \rangle = 1 \quad (38)$$

Furthermore, we can express an effective diffusivity tensor \mathbf{D}^{eff} as:

$$\mathbf{D}^{\text{eff}} = \langle \beta(\mathbf{I} + \nabla_{\mathbf{y}} \chi + \text{Pe} \mathbf{V}^* \chi - \text{Pe} \mathbf{v}^+ \chi) \rangle \quad (39)$$

However, it was shown [10] that the symmetric part of \mathbf{D}^{eff} can be also expressed as:

$$\mathbf{D}^{\text{eff}} = \langle \beta(\mathbf{I} + \nabla_{\mathbf{y}} \chi)(\mathbf{I} + \nabla_{\mathbf{y}} \chi)^T \rangle \quad (40)$$

In fact, the full form of the effective diffusion tensor is irrelevant since its effect on the homogenised solution is defined by its product with the Hessian matrix $\nabla_{\mathbf{x}}^2 w_0$, so that only its symmetric part contributes. It is thus more convenient to express it in symmetric form. Physically this means that all the correction due to the microscale velocity is concealed in χ , and it does not require to be accounted for further in \mathbf{D}^{eff}

Finally, we include the effect of the exponential term in the decomposition of w , we transform back the drifted spatial coordinate, and we let $\varepsilon \rightarrow 0$ to obtain the homogenised equation for $\omega(\mathbf{x}, t) = \omega_0(\mathbf{x}, t) + \mathcal{O}(\varepsilon)$:

$$\frac{\partial \omega}{\partial t} + \nabla_{\mathbf{x}} \cdot (\text{Pe}_L \mathbf{V}^* \omega - \mathbf{D}^{\text{eff}} \cdot \nabla_{\mathbf{x}} \omega) = -\lambda \omega \quad (41)$$

Where we introduced the macroscopic Péclet number $\text{Pe}_L = UL/\mathcal{D} = \text{Pe}/\varepsilon$, which is evaluated at the macroscale. It should be noted that equation (41) is not immediately equivalent to the equation for the average concentration $\langle c \rangle$. In fact:

$$\langle c \rangle = \langle \phi \omega \rangle = \frac{1}{\varepsilon} \int_{\mathcal{Y}_f} \phi(\mathbf{y}) \omega(\mathbf{x}, \mathbf{y}, t) d\mathbf{y} \quad (42)$$

However, employing expansion (26) and letting $\varepsilon \rightarrow 0$, as we did to obtain the macroscopic equation (41) and $\omega(\mathbf{x}, t)$, we obtain:

$$\langle c \rangle = \frac{1}{\varepsilon} \int_{\mathcal{Y}_f} \phi(\mathbf{y}) \omega(\mathbf{x}, t) d\mathbf{y} = \langle \phi \rangle \omega_0(\mathbf{x}, t) + \mathcal{O}(\varepsilon) \quad (43)$$

Finally, taking a ϕ normalised over the fluid volume we can write the asymptotic limit:

$$\langle c \rangle \sim \omega_0(\mathbf{x}, t), \quad \varepsilon \rightarrow 0. \quad (44)$$

And we rewrite the macroscopic equation for the first order approximation of $\langle c \rangle$:

$$\frac{\partial \langle c \rangle}{\partial t} + \nabla \cdot (\text{Pe}_L \mathbf{V}^* \langle c \rangle - \mathbf{D}^{\text{eff}} \cdot \nabla \langle c \rangle) = -\lambda \langle c \rangle \quad (45)$$

Remark 2. *The fact that we took the limit $\varepsilon \rightarrow 0$ is equivalent to state that we employed a local perturbation analysis in this work. This has the consequence that equation 45 is expected to be valid only in the case in which the microscopic and macroscopic scales are totally separated and $\ell \ll L$.*

Alternatively, one can retain terms up to $\mathcal{O}(\varepsilon^2)$ and merely consider equation (41) as the equation for w_0 , i.e. the leading order term. The average concentration can be corrected introducing a first order term:

$$\langle c \rangle = \omega_0 + \varepsilon \langle \phi \chi \rangle \cdot \nabla \omega_0 + \mathcal{O}(\varepsilon^2), \quad \varepsilon < 1 \quad (46)$$

equation 46 is often referred as the “first corrector equation” [9].

2.4. Extension to inhomogeneous boundary conditions

In Section 2.1, we employed the homogeneity of the Robin boundary condition to define an eigenvalue problem for ϕ , which allows to evaluate the eigenvalue λ . Thus, our approach, in the present formulation, fails when considering generic inhomogeneous boundary conditions, i.e. when $g = g(\mathbf{x}, \mathbf{y}, t)$. However, the method can still be exploited when the inhomogeneous term is a function of \mathbf{x} and \mathbf{y} only through c and its gradient:

$$g = g(c, \nabla c \cdot \mathbf{n}) = a(c - c_T) + b \nabla c \cdot \mathbf{n} \quad (47)$$

Specially, one can write the boundary condition on Γ in the more familiar form:

$$\nabla c \cdot \mathbf{n} = -\text{Da}_{\Pi}^* (c - c_{\Gamma}), \quad \text{Da}_{\Pi}^* = \frac{(\kappa - a)\ell}{D - b}, \quad b \neq \mathcal{D}, \quad (48)$$

Which gives the inhomogeneous Dirichlet boundary condition:

$$c = c_{\Gamma}, \quad c_{\Gamma} = \frac{d}{\kappa - a}, \quad b = \mathcal{D} \quad (49)$$

In case the inhomogeneous term is in the form given in equation 47, the linearity of advection-diffusion allows to define a new dimensionless concentration:

$$c'(\mathbf{x}) = c(\mathbf{x}, t) - c_{\Gamma} \quad (50)$$

Which satisfies our initial homogeneous problem. Thus, the analysis remains valid when the inhomogeneity can be expressed as an additive constant to the field c .

Notice that this method fails in case of inhomogeneous Neumann boundary conditions or in case of more general expressions for g .

However, c_{Γ} can still be a function of the macroscopic coordinate alone and vary only at large scales

3. Numerical implementation of the upscaling method

We employ the C++ opensource finite volume library OpenFOAM[®] [21] for implementing a numerical solver that performs the upscaling procedure in general geometries. We motivate our choice of OpenFOAM[®] over other libraries with its wide diffusion in both academic and industry, and with the wide range of classes already available in the library and structured in an consistent object-oriented programming approach.

3.1. Overall structure of the algorithm

Figure 1 illustrates the overall algorithms, which consists on two main sequential operations:

- i Solving the spectral cell problem for the Eigenvalue and ajoint problems.
- ii Solving the cell corrector problem for the first order corrector χ .

As input, the algorithm requires an appropriate velocity field which can be obtained from native OpenFOAM[®] solver such as `simpleFoam`.

3.2. Power method for the spectral problem

Solving the spectral problems poses an additional complication with respect to standard power methods: the Eigenvalue and adjoint problems are coupled through λ .

We propose an iterative segregated algorithm where coupling of λ is only achieved through residual control. At each iteration n , the values of fields and eigenvalues at iteration $n + 1$ are calculated following a series of steps:

1. Compute ϕ^{n+1} and $\phi^{\dagger, n+1}$ from:

$$\phi^{n+1} = \mathcal{L}^{-1} (\lambda^n \phi^n), \quad (51)$$

$$\phi^{\dagger, n+1} = (\mathcal{L}^{\dagger})^{-1} (\lambda^{\dagger, n} \phi^{\dagger, n}). \quad (52)$$

This operation may consist in two sets of iterations: solution of the linear systems and corrections for the non-orthogonal fluxes. Notice that we introduced the adjoint eigenvalue λ^{\dagger} , which should tend to λ for $n \rightarrow \infty$.

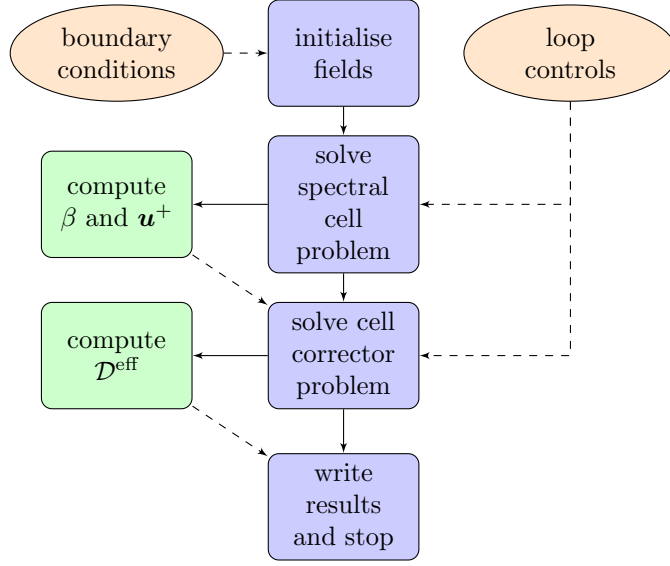


Figure 1: Overview of the numerical procedure. Orange clouds indicate that data is read from OpenFOAM® dictionaries, blue boxes indicate operations and green boxes indicate the computation of quantities relevant to subsequent operations. Dashed lines represent flow of information.

2. Update the eigenvalues using the Rayleigh quotient:

$$\lambda^{n+1} = \lambda^n \frac{\langle \phi^n \phi^n \rangle}{\langle \phi^{n+1} \phi^n \rangle}, \quad \lambda^{\dagger, n+1} = \lambda^{\dagger, n} \frac{\langle \phi^{\dagger, n} \phi^{\dagger, n} \rangle}{\langle \phi^{\dagger, n+1} \phi^{\dagger, n} \rangle}. \quad (53)$$

3. Normalise ϕ^{n+1} and $\phi^{\dagger, n+1}$:

$$\phi^{n+1} = \frac{\phi^{n+1}}{\langle \phi^{n+1} \rangle}, \quad \phi^{\dagger, n+1} = \frac{\phi^{\dagger, n+1}}{\langle \phi^{\dagger, n+1} \rangle}, \quad (54)$$

Notice that this normalisation is arbitrary and we will later re-normalise $\phi^{\dagger, n+1}$ to be consistent with equation 38.

4. Check convergence against a number of norms with user-defined tolerances. We choose to test both the residuals for ϕ and ϕ^{\dagger} defined as:

$$\text{res}(\phi^{n+1}) = \max\left(\frac{|\phi^{n+1}| - |\phi^n|}{|\phi^n|}\right), \quad \text{res}(\phi^{\dagger, n+1}) = \max\left(\frac{|\phi^{\dagger, n+1}| - |\phi^{\dagger, n}|}{|\phi^{\dagger, n}|}\right), \quad (55)$$

Where max is the maximum and the operator $|\cdot|$ denotes the absolute value. Clearly, the error on the eigenvalues is also a critical metrics to assess convergence:

$$(\lambda\text{-error})^{n+1} = \frac{|\lambda^{\dagger, n+1} - \lambda^{n+1}|}{\lambda^{n+1}}. \quad (56)$$

When all the metrics pass the convergence test (generally their value should be smaller than 10^{-5}), the spectral solver exits the loop.

After convergence, the eigenfunctions need to be re-normalised to satisfy $\langle \phi \rangle = 1$ and $\langle \beta \rangle = 1$ to be consistent with our formulations. While no action needs to be taken for ϕ , ϕ^{\dagger} is finally re-scaled simply dividing it by $\langle \phi^{\dagger} \phi \rangle$.

3.3. Numerical solution of the corrector problem

Finally, the corrector problem is also solved iteratively to correct for non-orthogonal fluxes. Furthermore, χ is gauge-invariant, in the sense that is defined up to a constant. From equation 44, we notice that our approximation of $\langle c \rangle$ is of order $\mathcal{O}(\varepsilon^2)$ when $\langle \phi \chi \rangle = 0$. Thus, at each iteration n we impose:

$$\chi^{n+1} = \chi^{n+\frac{1}{2}} - \langle \phi \chi^{n+\frac{1}{2}} \rangle, \quad (57)$$

where $\chi^{n+\frac{1}{2}}$ is calculated from the solution of the corrector problem before the gauge scaling.

4. Numerical results

4.1. Verification

We verify both our code and the upscaling methodology by direct comparison with spatial averaged data from fully resolved pore-scale simulations. Flow and scalar transport are solved in two dimensions for an array of 26 face-centred-cubic (FCC) cells (see Fig. 2) using the OpenFOAM® native solvers *simpleFoam* (classic Navier-Stokes solver employing the SIMPLE algorithm for pressure-velocity coupling) and *scalarTransportFoam* (standard advection-diffusion equation corresponding to equation 1). Notice that FCC configurations are a standard idealisation of porous media [22]. When solving equation 1 at the pore-scale, we provide the following external boundary conditions:

$$c(x=0, y) = 1, \quad \left. \frac{\partial c}{\partial x} \right|_{x=L} = 0, \quad (58)$$

where x is the axial direction of the cell array and L is the domain length. We ensure the flow is in Stokes (viscous) regime by imposing a value of the Reynolds number $\text{Re} < 10^{-3}$ everywhere.

Steady-state results are then averaged over each cell and compared against prediction from the ordinary differential equation (ODE):

$$\frac{d}{dx} \left(V_x^* \langle c \rangle - \mathcal{D}_{xx}^{\text{eff}} \frac{d\langle c \rangle}{dx} \right) = -\lambda \langle c \rangle, \quad (59)$$

where V_x^* is the effective velocity in x and $\mathcal{D}_{xx}^{\text{eff}}$ is the axial component of the effective diffusivity tensor. Choosing appropriate boundary conditions for equation 59 is not trivial, since we do not know the value of $\langle c \rangle$ at $x = 0$. However, since our only objective is to evaluate the accuracy of this method, we just impose:

$$\langle c \rangle(x=0) = 1, \quad \left. \frac{d\langle c \rangle}{dx} \right|_{x=L} = 0, \quad (60)$$

and compare the results against fully developed (i.e., far from the inlet) pore-scale simulations with an appropriate rescaling. Therefore, all comparisons will be made dividing all values of $\langle c \rangle$ obtained from pore-scale simulations with the value of $\langle c \rangle$ at the 10^{th} FCC cell, where the profile of c is well developed for all the simulations.

Equation 59 is solved to spectral accuracy using the MATLAB® package *Chebfun* [23].

We compute the coefficients in equation 59 using our novel solver from a single FCC cell. Fig. 3 shows the relevant fields arising from the solution of the cell problem. Notice that the eigenfunction ϕ is Fig. 3a and the adjoint ϕ^\dagger in Fig. 3b only differ for the direction of the advective component as expected from inspection of their governing equation.

Results from two pore-scale simulations are compared with solutions of equation 59 in Fig 4. Overall, the upscaling method provides excellent results, with little deviations from the pore-scale simulations. Notice that such agreement was obtained by rescaling the cell average concentration from the pore-scale simulations by an appropriate reference value (i.e., the value of an FCC cell in the asymptotic regime). Using this approach, we were able to test the accuracy of the method without an a complete knowledge of the external boundary conditions.

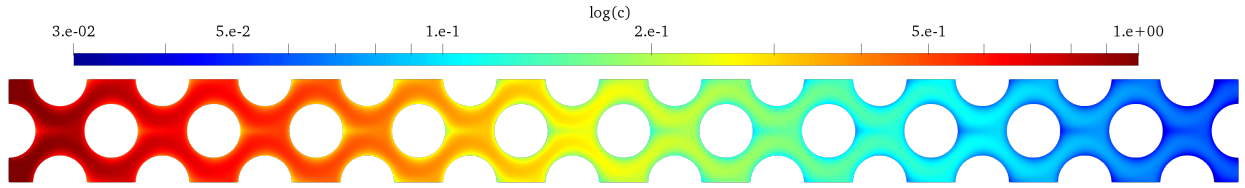


Figure 2: Example results from a two-dimensional pore-scale simulation. For clarity, we show only a fraction of the FCC cells composing the computational domain.

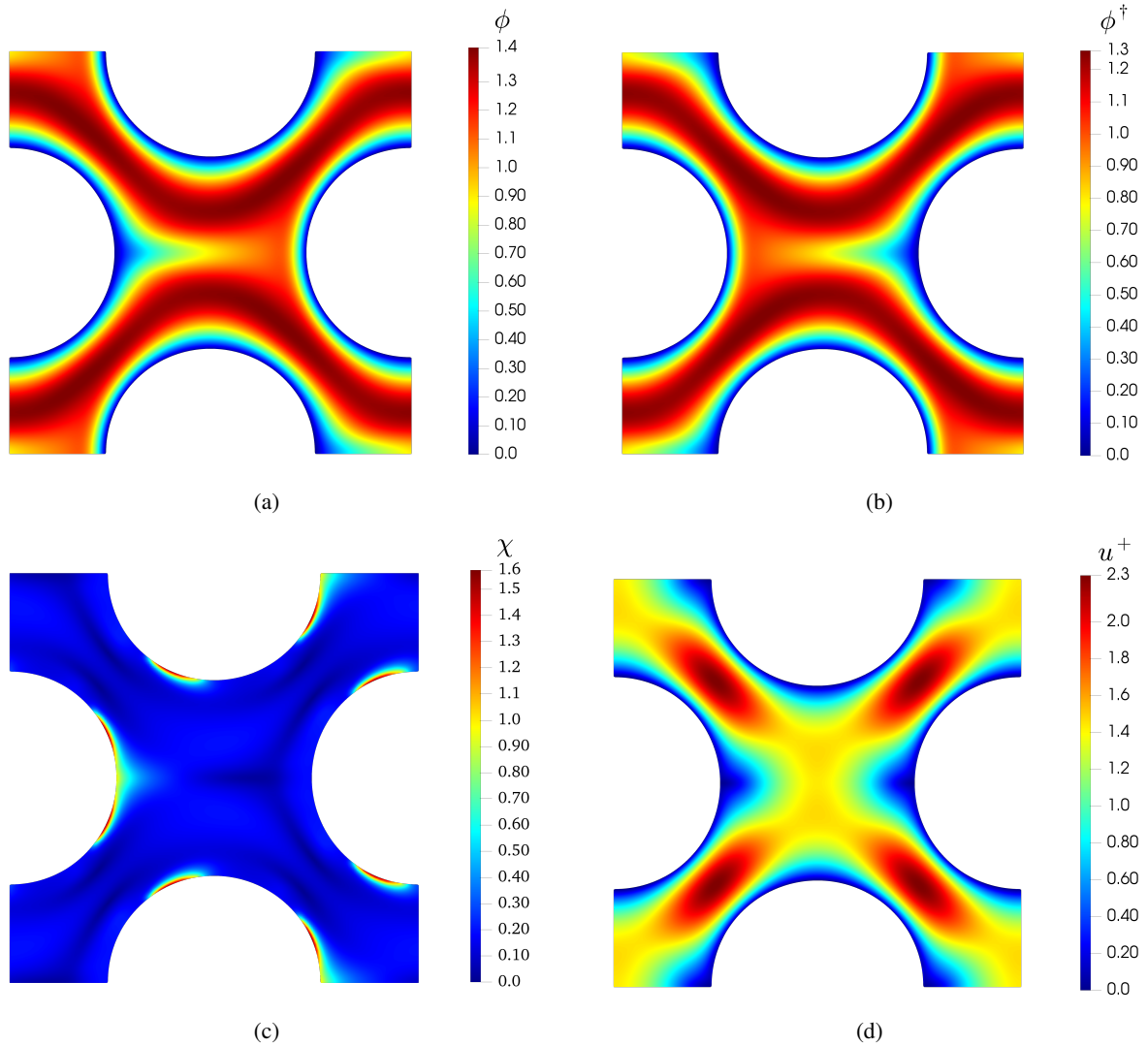


Figure 3: Results from the spectral and first order corrector solver for the FCC cell in the case $Pe = 100$, $\epsilon = 0.7$ and $Da_{II} = 962$. u^+ is the magnitude of \mathbf{u}^+ and χ is the magnitude of χ .

4.2. Parametric study - homogenisation of flow through reactive FCC array of spheres

We illustrate how the present method can be applied to large scale studies by studying the effect of Pe and Da_{II} on the effective parameters of the homogenised transport equation. Results are presented in Figures 5, 6 and 7 for different

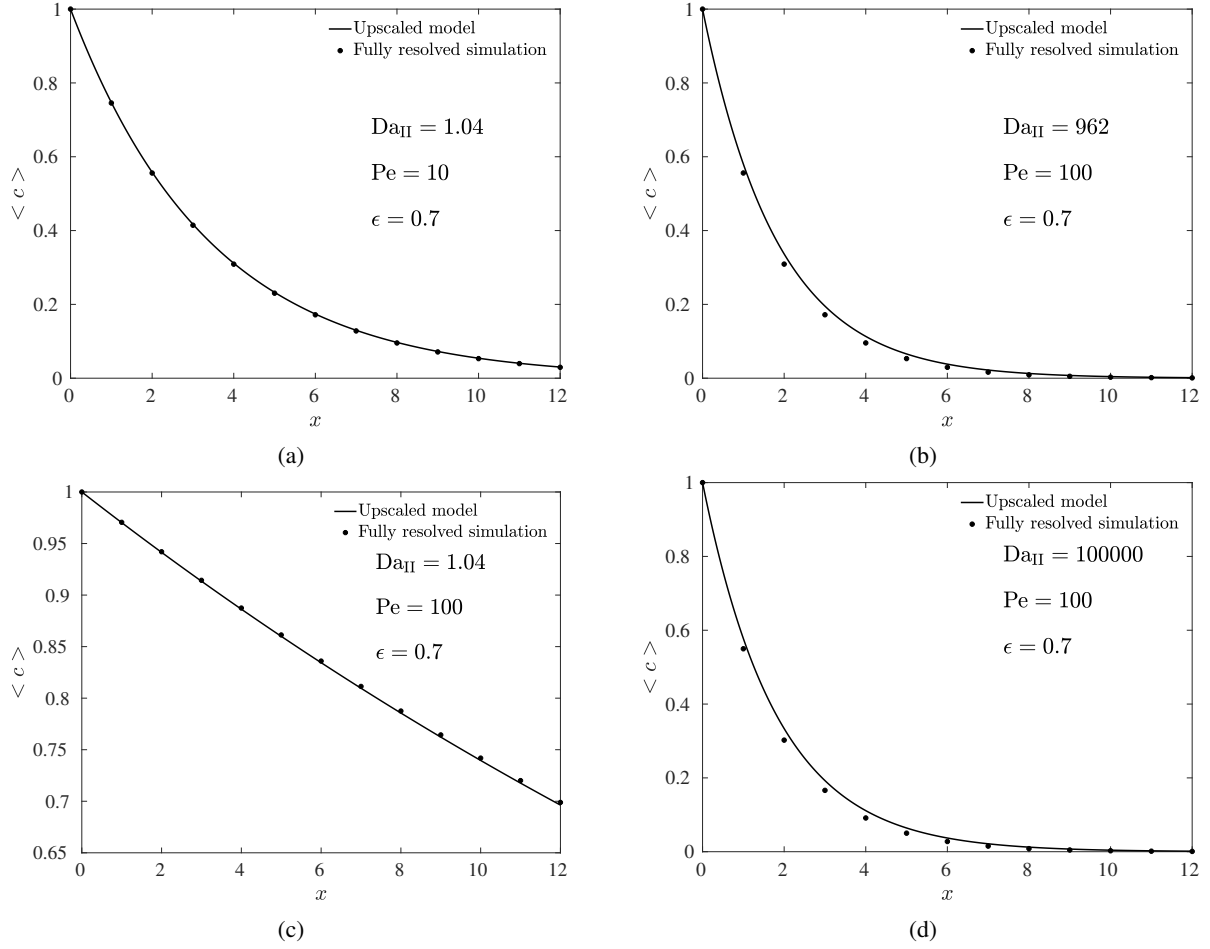


Figure 4: Comparison of results from equation 59 against resolved pore-scale simulations. Here, x is scaled with the length of an FCC cell such that the value of x corresponds to the number of FCC cells.

porosities ϵ . Furthermore, full numerical results are provided in the additional material.

We probe the range $Da_{II} \in [10^{-2}, 10^5]$ in order to capture both the limits tending to Neumann and Dirichlet boundary conditions. Effective parameters are scaled based on such limits, defining the 'primed' effective parameters as:

$$\lambda' = \frac{\lambda - \lambda_N}{\lambda_D - \lambda_N}, \quad \mathbf{D}' = \frac{\mathbf{D}^{\text{eff}} - \mathbf{D}_N^{\text{eff}}}{\mathbf{D}_D^{\text{eff}} - \mathbf{D}_N^{\text{eff}}}, \quad \mathbf{V}' = \frac{\mathbf{V}^* - \mathbf{V}_N^*}{\mathbf{V}_D^* - \mathbf{V}_N^*}, \quad (61)$$

where the subscripts N and D indicate that the effective parameter has been calculated using Neumann or Dirichlet boundary conditions respectively. Notice that obviously $\lambda_D = 0$ since it does represent the non-reactive case.

Results from different values of ϵ show the little variation in the profiles of λ , but reveal interesting behaviours for both the effective dispersion and velocity.

Specifically, the effective dispersion profiles do not show any consistent trend with the Péclet number, which indicates the complex interconnection between this and the Damköhler number on the effective transport properties. However, it can be seen that both \mathcal{D}'_{xx} and \mathcal{D}'_{yy} tend to occupy a larger range of values with decreasing porosity. This can be explained considering that the flow field becomes more tortuous when larger portions of the domain are occupied by the solid phase. Interestingly, we notice that the effective diffusion coefficient in reactive systems can either higher or lower than that in non-reactive systems.

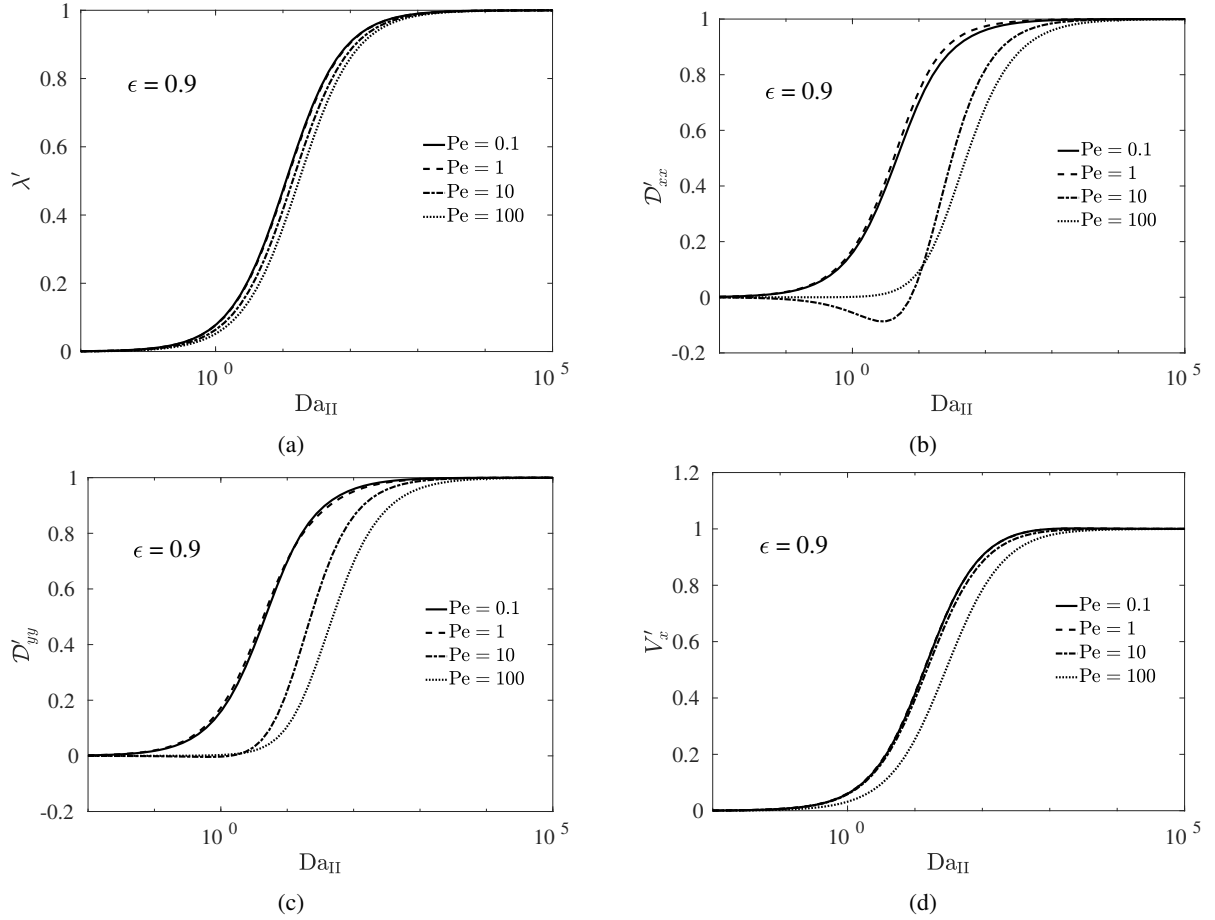


Figure 5: Scaled effective parameters as a function of the microscopic parameters for $\epsilon = 0.9$.

Another interesting feature predicted by this model, is a global minimum of the effective velocity in the range $Da_{II} \sim 10$ at high values of ϵ (maximum in V'_x). Such phenomenon is evident at low values of ϵ and Pe , where the effect of the reaction is stronger.

Overall, the results we presented lead to a better understanding of reactive flows through ordered arrays of cylinder and may provide useful hints for design of heat exchangers or catalysts.

5. Conclusions

In this work, we presented a methodology for the upscaling of reactive transport in porous media based on the works of Allaire and Raphael [3] and Mauri [4]. Such upscaling procedure has been described in details for homogeneous boundary condition and extended to simple non-homogeneous boundary conditions.

Furthermore, we implemented the method in the opensource library OpenFOAM® [21] and compared its predictions against fully resolved microscale simulations finding excellent agreement. This confirms the power and accuracy of homogenisation-based approaches to solve a range of 'closure problems'.

Finally, we presented a parametric study of reactive transport in ordered arrays of cylinders to illustrate the usage of the proposed method and numerical code. We found that the effective parameters depend on the Péclet and Damköhler

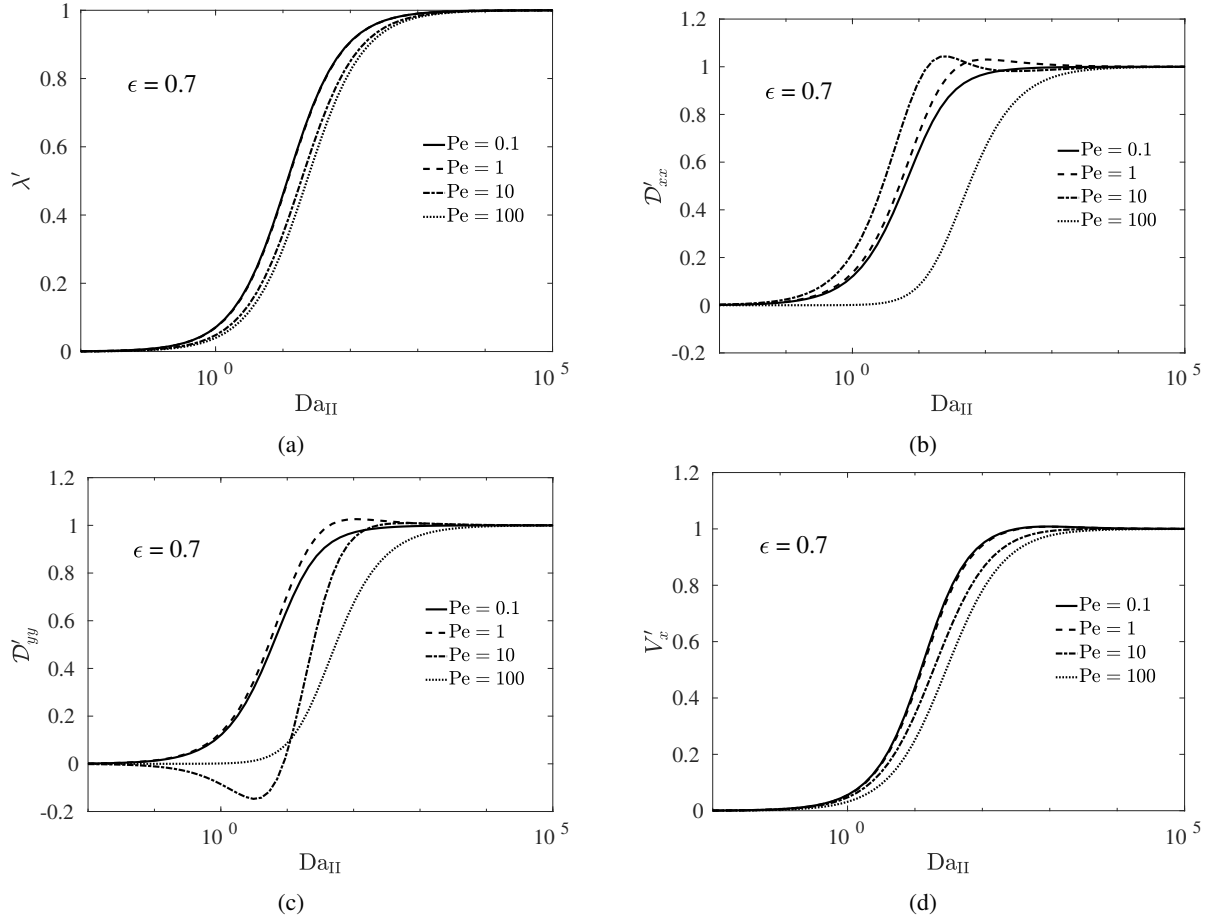


Figure 6: Scaled effective parameters as a function of the microscopic parameters for $\epsilon = 0.7$.

number in a complex manner and that the method is able to correctly recover the limiting cases of Dirichlet and Neumann boundary conditions.

While we restricted our numerical investigation to FCC configurations, the presented methodology and numerical code can be straightforwardly extended to any other geometry. In future works, we plan to use this method to study heat/mass transfer in random arrays of sphere and even homogeneous and wall bounded suspensions [24, 25].

From a theoretical point of view, future extension will also include the application to more complex, non-linear and electrokinetic boundary conditions [26]. These have important applications for electrokinetic energy conversion in nanofluidic channels [27].

As a final remark, we stress the fact we made our numerical code open source and freely available. This with the objective of extending the use of homogenisation-based techniques to a wider community and providing an 'upscaling toolbox' with solid mathematical foundations.

Acknowledgements

This work has been funded by the European Union's Horizon 2020 research and innovation programme, grant agreement number 764531, "SECURE – Subsurface Evaluation of Carbon capture and storage and Unconventional risks".

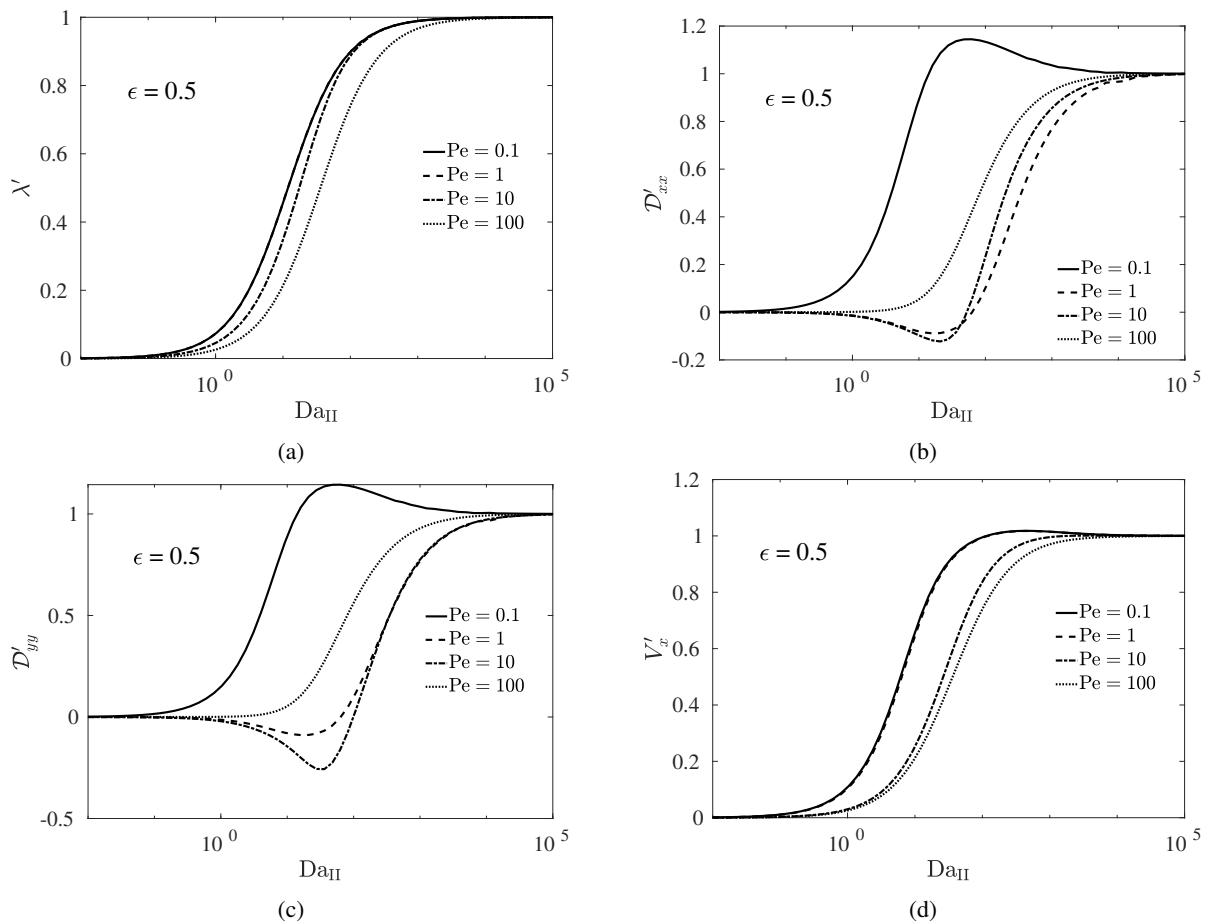


Figure 7: Scaled effective parameters as a function of the microscopic parameters for $\epsilon = 0.5$.

References

- [1] F. Valdés-Parada, C. Aguilar-Madera, J. Álvarez-Ramírez, *Chemical Engineering Science* 66 (2011) 2177 – 2190.
- [2] I. Battiato, D. Tartakovsky, *Journal of Contaminant Hydrology* 120-121 (2011) 18 – 26. Reactive Transport in the Subsurface: Mixing, Spreading and Reaction in Heterogeneous Media.
- [3] G. Allaire, A.-L. Raphael, *Comptes Rendus Mathématique* 344 (2007) 523 – 528.
- [4] R. Mauri, *Physics of Fluids A: Fluid Dynamics* 3 (1991) 743–756.
- [5] A. H.-D. Cheng, in: *Theory and Applications of Transport in Porous Media*, volume 27, Springer International Publishing, 2016, pp. 703–773.
- [6] S. Radl, F. Municchi, *Advances in Chemical Engineering* 53 (2018) 153–237.
- [7] M. Kardar, *Statistical Physics of Fields*, Cambridge University Press, 2007.
- [8] G. A. Pavliotis, A. M. Stuart, *Multiscale methods : averaging and homogenization*, Springer, 2008.
- [9] Y. Davit, C. G. Bell, H. M. Byrne, L. A. Chapman, L. S. Kimpton, G. E. Lang, K. H. Leonard, J. M. Oliver, N. C. Pearson, R. J. Shipley, S. L. Waters, J. P. Whiteley, M. Quintard, *Advances in Water Resources* 62 (2013) 178–206.
- [10] J. Auriault, *International Journal of Engineering Science* 29 (1991) 785 – 795.
- [11] J.-L. Auriault, P. Adler, *Advances in Water Resources* 18 (1995) 217–226.
- [12] I. Battiato, D. Tartakovsky, *Journal of contaminant hydrology* 120 (2011) 18–26.
- [13] G. Boccardo, E. Crevacore, R. Sethi, M. Icardi, *Journal of contaminant hydrology* 212 (2018) 3–13.
- [14] F. Municchi, M. Icardi, arXiv preprint arXiv:1906.01316 (2019).
- [15] A. Fadili, P. M. Tardy, J. A. Pearson, in: *IUTAM Symposium on Asymptotics, Singularities and Homogenisation in Problems of Mechanics*, Springer, pp. 351–361.
- [16] M. Cherdantsev, K. Cherednichenko, I. Velčić, *Applicable Analysis* 98 (2019) 91–117.
- [17] M. Icardi, G. Boccardo, R. Tempone, *Advances in Water Resources* 95 (2016) 46–60.
- [18] T. L. van Noorden, A. Muntean, *European Journal of Applied Mathematics* 22 (2011) 493–516.
- [19] D. L. Brown, P. Popov, Y. Efendiev, *GEM-International Journal on Geomathematics* 2 (2011) 281.
- [20] G. Allaire, *Asymptotic Analysis* 2 (1989) 203–222.

- [21] T. O. Foundation (2014) 4–5.
- [22] E. Crevacore, T. Tosco, R. Sethi, G. Boccardo, D. L. Marchisio, *Physical Review E* 94 (2016) 053118.
- [23] T. A. Driscoll, N. Hale, L. N. Trefethen, *Chebfun guide*, Pafnuty publications, 2014.
- [24] F. Municchi, S. Radl, *International Journal of Heat and Mass Transfer* 111 (2017) 171–190.
- [25] F. Municchi, S. Radl, *International Journal of Heat and Mass Transfer* 120 (2018).
- [26] V. Joekar-Niasar, L. Schreyer, M. Sedighi, M. Icardi, J. Huyghe, *Transport in Porous Media* (????) 1–32.
- [27] Y. Ren, D. Stein, *Nanotechnology* 19 (2008) 195707.